



The association between lacunes and white matter hyperintensity features on MRI: The SMART-MR study

Rashid Ghaznawi^{1,2}, Mirjam I Geerlings², Myriam G Jaarsma-Coes^{1,3} , Maarten HT Zwartbol¹, Hugo J Kuijf⁴ , Yolanda van der Graaf², Theo D Witkamp¹, Jeroen Hendrikse¹ and Jeroen de Bresser^{1,3}; on behalf of the SMART Study Group*

Abstract

Lacunes and white matter hyperintensities (WMHs) are features of cerebral small vessel disease (CSVD) that are associated with poor functional outcomes. However, how the two are related remains unclear. In this study, we examined the association between lacunes and several WMH features in patients with a history of vascular disease. A total of 999 patients (mean age 59 ± 10 years) with a 1.5 T brain magnetic resonance imaging (MRI) scan were included from the SMART-MR study. Lacunes were scored visually and WMH features (volume, subtype and shape) were automatically determined. Analyses consisted of linear and Poisson regression adjusted for age, sex, and total intracranial volume (ICV). Patients with lacunes ($n = 188$; 19%) had greater total ($B = 1.03$, 95% CI: 0.86 to 1.21), periventricular/confluent ($B = 1.08$, 95% CI: 0.89 to 1.27), and deep ($B = 0.71$, 95% CI: 0.44 to 0.97) natural log-transformed WMH volumes than patients without lacunes. Patients with lacunes had an increased risk of confluent type WMHs ($RR = 2.41$, 95% CI: 1.98 to 2.92) and deep WMHs ($RR = 1.41$, 95% CI: 1.22 to 1.62) and had a more irregular shape of confluent WMHs than patients without lacunes, independent of total WMH volume. In conclusion, we found that lacunes on MRI were associated with WMH features that correspond to more severe small vessel changes, mortality, and poor functional outcomes.

Keywords

Small vessel disease, lacunes, white matter hyperintensities, magnetic resonance imaging, cerebrovascular disease

Received 17 April 2018; Revised 14 July 2018; Accepted 2 August 2018

Introduction

Cerebral small vessel disease (CSVD) is a major cause of cognitive decline and dementia.^{1–3} Lacunes and white matter hyperintensities (WMHs) of presumed vascular origin are considered hallmark magnetic resonance imaging (MRI) features of CSVD and are frequently observed in older individuals.⁴ WMHs appear as hyperintense lesions on MRI in fluid-attenuated inversion recovery (FLAIR) images.⁵ Lacunes are round or ovoid, subcortical, fluid filled cavities of between 3 mm and 15 mm in diameter with a signal intensity similar to cerebrospinal fluid.⁵

CSVD is a highly prevalent disease in which the clinical spectrum can range from asymptomatic

¹Department of Radiology, University Medical Center Utrecht, Utrecht, the Netherlands

²Julius Center for Health Sciences and Primary Care, University Medical Center Utrecht, Utrecht, the Netherlands

³Department of Radiology, Leiden University Medical Center, Leiden, the Netherlands

⁴Image Sciences Institute, University Medical Center Utrecht, Utrecht, the Netherlands

*Listed in the 'Project members' section at the end of this article.

Corresponding author:

Mirjam I Geerlings, Julius Center for Health Sciences and Primary Care, University Medical Center Utrecht, P.O. Box 85500, Stratenum 6.131, 3508 GA Utrecht, the Netherlands.
Email: m.geerlings@umcutrecht.nl

disease through to vascular dementia.⁶ Previous histopathological studies have shown that WMHs correspond to different underlying brain parenchymal changes.⁷ Smooth, periventricular lesions are associated with mild, non-ischemic parenchymal changes.⁸ In contrast, irregular and confluent WMHs are associated with more severe brain parenchymal changes, including loss of myelin and incomplete parenchymal destruction.^{8–10} Functionally, confluent and deep WMHs are associated with cognitive impairment, gait disturbances, mortality, and a higher risk of stroke, while these associations have not been found for periventricular lesions.^{11–14} Lacunes, previously thought to arise solely from lacunar infarcts, are now considered lesions that may result from different causes, such as small hemorrhages, infarcts microembolism, and amyloid angiopathy.⁵ Importantly, there is increasing evidence that presence of lacunes on MRI is associated with cognitive impairment and poor clinical outcomes after stroke.^{15–17} The relationship between lacunes and WMH features, however, remains unclear. As lacunes can have profound clinical consequences, examining the relationship between the two may aid in identifying patients with certain WMH characteristics that are prone to develop lacunes.

To better define the relationship between lacunes and WMH features, we developed an automated method to assess different WMH features (volume, subtype, and shape) on brain MRI.¹⁸ With this method, we investigated the relationship between lacunes and WMH features in a large group of patients with a history of vascular disease.

Material and methods

Study population and study sample

Data were used from the Second Manifestations of ARterial disease-Magnetic Resonance (SMART-MR) study, a prospective cohort study at the University Medical Center Utrecht with the aim to investigate risk factors and consequences of brain changes on MRI in patients with symptomatic atherosclerotic disease.¹⁹ In brief, between 2001 and 2005, 1309 middle-aged and older adult persons newly referred to the University Medical Center Utrecht for treatment of symptomatic atherosclerotic disease (manifest coronary artery disease, cerebrovascular disease, peripheral arterial disease, or abdominal aortic aneurysm) were included for baseline measurements. During a one day visit to our medical center, a physical examination, ultrasonography of the carotid arteries to measure the intima-media thickness (IMT) (mm), blood and urine samplings, neuropsychological assessment, and a 1.5 T brain MRI scan were performed. The height and weight

of patients were measured, and the body mass index (BMI) (kg/m^2) was calculated. Questionnaires were used for the assessment of demographics, risk factors, medical history, medication use, and cognitive and physical functioning. The SMART-MR study was approved by the medical ethics committee of the University Medical Center Utrecht according to the guidelines of the Declaration of Helsinki of 1975 and written informed consent was obtained from all participants.

Of the 1309 patients included in the SMART-MR study, MRI data were irretrievable for 19 patients and 239 patients had missing data of one or more MRI sequences due to motion artifacts or logistic reasons. Of the remaining 1051 patients, 44 had unreliable brain volume data due to motion artifacts in all three MRI sequences, and four patients were excluded due to severe undersegmentation of WMHs by the automated segmentation program. Four patients were excluded because they did not have any WMHs greater than five voxels. As a result, 999 patients were included in the current study.

Cardiovascular risk factors

Smoking habits and alcohol intake were assessed with questionnaires and were categorized as never, former, or current. Height and weight were measured, and the BMI was calculated (kg/m^2). Systolic blood pressure (SBP) (mmHg) and diastolic blood pressure (DBP) (mmHg) were measured three times with a sphygmomanometer, and the average of these measures was calculated. Hypertension was defined as a mean SBP of ≥ 160 mmHg, a mean DBP of ≥ 95 mmHg, self-reported use of antihypertensive drugs, or a known history of hypertension at inclusion. An overnight fasting venous blood sample was taken to determine glucose and lipid levels. Diabetes mellitus was defined as the use of glucose-lowering drugs, a known history of diabetes mellitus, or a fasting plasma glucose level of > 11.1 mmol/l. Hyperlipidemia was defined as a total cholesterol of > 5.0 mmol/l, a low-density lipoprotein cholesterol of > 3.2 mmol/l, use of lipid-lowering drugs, or a known history of hyperlipidemia. Mean carotid IMT (in mm) was calculated for the left and right common carotid arteries based on six far-wall measurements on ultrasound.

MRI

MRI of the brain was performed on a 1.5 T whole-body system (Gyrosan ACS-NT, Philips Medical Systems, Best, the Netherlands) using a standardized scan protocol consisting of two-dimensional multi-slice sequences. Transversal T1-weighted (gradient-echo; repetition

time (TR)=235 ms; echo time (TE)=2 ms), T2-weighted (turbo spin-echo; TR=2200 ms; TE=11 ms), FLAIR (turbo spin-echo; TR=6000 ms; TE=100 ms; inversion time (TI)=2000 ms), and T1-weighted inversion recovery images (turbo spin-echo; TR=2900 ms; TE=22 ms; TI=410 ms) were acquired. All MR sequences had a resolution of $1.0 \times 1.0 \times 4.0 \text{ mm}^3$ and consisted of 38 contiguous slices (field of view $230 \text{ mm} \times 230 \text{ mm}$; matrix size 180×256 , slice gap 0 mm).

Lacunae were visually rated by a neuroradiologist (TW) blinded to patient characteristics on the T1-weighted, T2-weighted, and FLAIR images. We defined lacunae as focal lesions between 3 to 15 mm according to the STRIVE criteria.⁵ Brain infarcts were visually rated by a neuroradiologist (TW) blinded to patient characteristics on the T1-weighted, T2-weighted and FLAIR images.

Assessment of WMH volumes and other brain volumes

WMH volumes were obtained using an automated segmentation program on the T1-weighted, FLAIR, and T1-weighted inversion recovery sequences of the MR scans. A probabilistic segmentation technique was performed with *k*-nearest neighbor classification,²⁰ distinguishing gray matter, white matter, cerebrospinal fluid, and lesions. Cerebral infarcts, including lacunae and their hyperintense rim, were manually segmented. WMH segmentations were visually checked by an investigator (RG) using an image processing framework (MeVisLab 2.7.1., MeVis Medical Solutions AG, Bremen, Germany) to ensure that all cerebral infarcts were correctly removed from the WMH segmentations. Incorrectly segmented voxels were automatically added to the correct segmentation volumes. Next, ventricle segmentation was performed using the fully automated lateral ventricle delineation (ALVIN) algorithm²¹ in Statistical Parametric Mapping 8 (SPM8, Wellcome Trust Centre for Neuroimaging, University College London, London, UK) for Matlab (The MathWorks, Inc., Natick, MA, United States). The ALVIN mask was used to determine the margins of the lateral ventricles. A threshold of 10% was applied to the WMH probability maps to obtain binary data. A group of voxels was considered a WMH lesion if their faces, edges or corners touched along either one, two or all three of the primary axes (26-connectivity rule). WMHs were labeled based on their continuity with the margins of the lateral ventricle and the extension from the lateral ventricle into the white matter. We defined periventricular WMHs as lesions contiguous with the margins of the lateral ventricles and extending up to and including 10 mm from

the lateral ventricle into the white matter. Confluent WMHs were defined as lesions contiguous with the margins of the lateral ventricles and extending more than 10 mm from the lateral ventricles into the white matter. Deep WMHs were defined as lesions that were separated from the margins of the lateral ventricles, regardless of their distance to the margins of the lateral ventricles. Total WMH volume was defined as the sum of periventricular or confluent WMHs and all deep WMHs. Examples of periventricular, confluent, and deep WMHs visualized in our algorithm are shown in Figure 1. The automatically assigned lesion labels were visually checked by an investigator (MGJC) and manually corrected if necessary.

Total brain volume was calculated by summing the volumes of gray matter, white matter, total WMH and, if present, the volumes of brain infarcts.¹⁹ Total ICV was calculated by summing the cerebrospinal fluid volume and total brain volume.

Assessment of WMH subtypes

To assess whether different WMH subtypes were associated with lacunae, patients were categorized into the following three WMH subtypes: periventricular WMHs without deep WMHs, periventricular WMHs with deep WMHs, and confluent WMHs. The rationale behind the WMH subtype definitions is described in the Supplementary material.

Assessment of WMH shape

We assessed WMH shape using shape features.¹⁸ WMH shape features were calculated from the binary segmentation data for all patients. Definitions and selection of shape features are described in the Supplementary material and Supplementary Table 1. In short, we analyzed periventricular and confluent WMHs by reconstructing convex hulls and calculating volume and surface area ratios. Solidity was obtained by dividing lesion volume by the volume of its convex hull, while convexity was obtained by dividing the convex hull surface area by the lesion's surface area. The concavity index²² was calculated from the solidity and convexity. A mean value for solidity, convexity, and concavity index was calculated for each patient. For deep WMHs, we calculated eccentricity by dividing the minor axis of a lesion by its major axis. In case of multiple deep WMHs, a mean value for eccentricity was calculated across all deep WMHs per patient. Fractal dimension was calculated for periventricular, confluent, and deep WMHs using the box counting method. A mean value for fractal dimension was calculated for periventricular or confluent WMHs and deep WMHs for each patient. Examples of WMHs that correspond

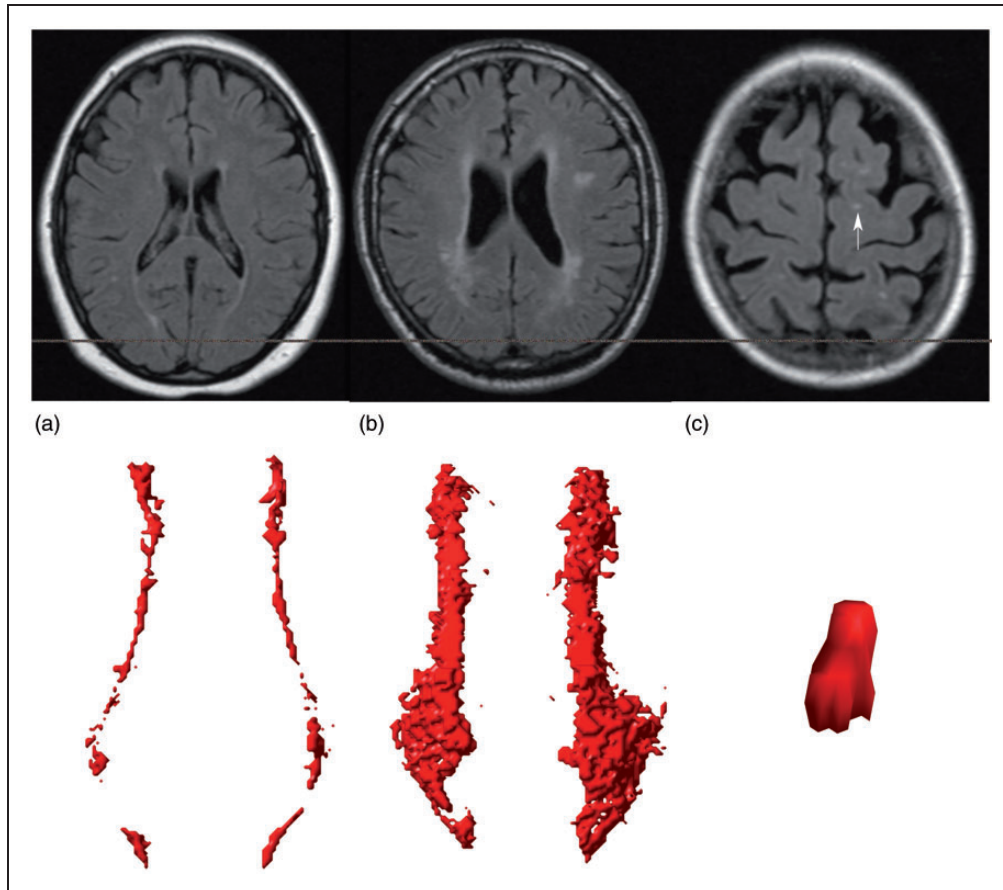


Figure 1. Examples of periventricular (a), confluent (b) and deep (c) WMHs visualized in our algorithm. The corresponding FLAIR images are shown. The deep WMH lesion (arrow) is reconstructed in the coronal view, while the periventricular and confluent WMHs are viewed from a transverse perspective.

to a low or high value of WMH shape features are shown in Supplementary Table 2.

Statistical analysis

First, baseline characteristics and WMH features (volume, subtype, and shape) of patients with lacunes and patients without lacunes were compared using an independent samples t-test or Chi-square test.

Second, linear regression analyses were performed to compare total, periventricular or confluent, and deep WMH volumes (natural log-transformed) in patients with lacunes versus patients without lacunes, adjusted for age, sex, and ICV. These analyses were repeated in patients with one lacune versus patients with multiple lacunes.

Third, relative risks for a confluent WMH subtype or a periventricular WMH subtype with deep WMHs were estimated using Poisson regression with robust error variance for patients with lacunes compared to patients without lacunes, adjusted for age, sex, and ICV. These analyses were

repeated in patients with one lacune versus patients with multiple lacunes. A periventricular WMH subtype without deep WMHs was chosen as the reference category.

Fourth, we assessed the association between lacunes and WMH shape features. Due to inherent shape differences between periventricular and confluent WMHs visible on MRI, analyses were performed across strata of three WMH subtypes (periventricular without deep WMHs ($n=360$), periventricular with deep WMHs ($n=424$), and confluent WMH ($n=215$)). Z-scores were calculated for the WMH shape features to facilitate the comparison between these features. Linear regression analyses were performed with presence of lacunes as independent variable and shape descriptor Z-scores as dependent variable. In the first model, we adjusted for age and sex. In the second model, we additionally adjusted for total WMH volume (%ICV) to assess to what extent the observed relationships were explained by WMH volume. The linear regression analyses were repeated in patients with one lacune versus patients with multiple lacunes.

A p -value of <0.05 was considered to be statistically significant. SAS 9.4 (SAS Institute, Cary, NC, USA) and SPSS 21.0 (Chicago, IL, USA) were used to analyze our data.

Results

Baseline characteristics for patients with lacunes ($n=188$; 19%) and without lacunes ($n=811$; 81%), and for the total study sample ($n=999$) are shown in Table 1. A total number of 439 lacunes were scored in 188 patients (range: 1 to 12 lacunes per patient). Eighty-six patients (9%) showed one lacune on MRI, while 102 patients (10%) showed multiple lacunes on MRI. Of the patients with multiple lacunes, the majority (72%) showed two or three lacunes on MRI.

Patients with lacunes were older ($p < 0.0001$), more often had diabetes mellitus ($p = 0.006$) and hypertension ($p < 0.0001$), had a higher IMT ($p < 0.0001$), but also had a lower BMI compared to patients without lacunes ($p = 0.02$). WMH features of patients with lacunes, patients without lacunes, and of the total study population are shown in Table 2. Patients with lacunes showed greater WMH volumes and were more likely to have a confluent WMH subtype than patients without lacunes ($p < 0.0001$). In patients with lacunes, periventricular and confluent WMHs showed a lower solidity ($p < 0.0001$) and higher fractal dimension ($p < 0.0001$) than patients without lacunes.

Association between lacunes and WMH volumes

The results of the linear regression analyses with total, periventricular or confluent, and deep WMH volumes

(natural log transformed) as dependent variables and lacunes as independent variable are shown in Table 3. After adjusting for age, sex, and total intracranial volume, patients with lacunes had greater total ($B = 1.03$, 95% CI: 0.86 to 1.21), periventricular or confluent ($B = 1.08$, 95% CI: 0.89 to 1.27), and deep ($B = 0.71$, 95% CI: 0.44 to 0.97) WMH volumes than patients without lacunes. Patients with multiple lacunes had greater total ($B = 0.36$, 95% CI: 0.05 to 0.67) and periventricular or confluent ($B = 0.37$, 95% CI: 0.03 to 0.70) WMH volumes than patients with one lacune; however no significant difference was found for deep WMH volumes ($B = -0.08$, 95% CI: -0.54 to 0.39).

Association between lacunes and WMH subtypes

Patients with lacunes had an increased risk of a confluent WMH subtype or a periventricular WMH subtype with deep WMHs than patients without lacunes (RR = 2.41, 95% CI: 1.98 to 2.92, RR = 1.41, 95% CI: 1.22 to 1.62, respectively), after adjusting for age, sex, and total ICV (Table 4). Patients with multiple lacunes did not show an increased risk of a confluent WMH subtype or a periventricular WMH subtype with deep WMHs than patients with one lacune (RR = 1.13, 95% CI: 0.93 to 1.36, RR = 1.20, 95% CI: 0.92 to 1.57, respectively).

Association between lacunes and WMH shape features

The results of the linear regression analyses of the associations between lacunes and WMH shape features are shown in Table 5.

Table 1. Baseline characteristics of the patients with lacunes, patients without lacunes, and the total study population.

	Patients with lacunes (n = 188)	Patients without lacunes (n = 811)	All patients (n = 999)	p^a
Age (years)	63 ± 10	58 ± 10	59 ± 10	<0.0001
Sex, % men	81	78	79	0.37
Cardiovascular risk factors				
BMI (kg/m ²)	26.2 ± 3.5	26.9 ± 3.8	26.7 ± 3.7	0.02
Smoking, % current	28	25	25	0.34
Alcohol intake, % current	76	74	74	0.72
Hypertension, %	67	48	51	<0.0001
Hyperlipidemia, %	79	78	79	0.99
Diabetes mellitus, %	27	18	20	0.006
IMT (mm)	1.04 ± 0.36	0.91 ± 0.29	0.93 ± 0.31	<0.0001 ^b

Note: Characteristics are presented as mean ± SD or %.

BMI: body mass index; IMT: intima-media thickness.

^a p -value of independent samples t-test or Chi-square test (if proportions) for comparison between patients with lacunes versus those without lacunes.

^bBetween group analysis was performed on natural log-transformed values due to a non-normal distribution of this characteristic.

Table 2. WMH features of patients with lacunes, patients without lacunes, and the total study population.

	Patients with lacunes (n = 188)	Patients without lacunes (n = 811)	All patients (n = 999)	p ^a
WMH volumes, ml ^b				
Total	2.9 (0.5, 18.1)	0.8 (0.2, 4.0)	0.9 (0.2, 6.4)	<0.0001 ^c
Periventricular or confluent	2.3 (0.4, 17.4)	0.6 (0.1, 3.3)	0.8 (0.1, 5.4)	<0.0001 ^c
Deep	0.2 (0.0, 1.2)	0.1 (0.0, 0.7)	0.1 (0.0, 0.8)	<0.0001 ^c
WMH subtypes on MRI, % ^d				
Periventricular	45	86	78	<0.0001
With deep	34	44	42	0.01
Without deep	11	42	36	<0.0001
Confluent	55	14	22	<0.0001
With deep	54	13	21	<0.0001
Without deep	1	1	1	0.22
WMH shape descriptors ^e				
Periventricular or confluent				
Solidity	0.40 ± 0.20	0.61 ± 0.25	0.57 ± 0.25	<0.0001
Convexity	1.07 ± 0.17	1.08 ± 0.16	1.07 ± 0.16	0.48
Concavity index	1.13 ± 0.16	1.04 ± 0.09	1.06 ± 0.11	<0.0001
Fractal dimension	1.41 ± 0.22	1.20 ± 0.20	1.24 ± 0.22	<0.0001
Deep				
Eccentricity	0.46 ± 0.12	0.49 ± 0.15	0.48 ± 0.14	0.004
Fractal dimension	1.45 ± 0.12	1.45 ± 0.16	1.45 ± 0.15	0.77

Note: Characteristics are presented as mean ± SD or %.

WMH: white matter hyperintensity; MRI: magnetic resonance imaging.

^ap-value of independent samples t-test or Chi-square test (if proportions) for comparison between the group with lacunes versus those without lacunes.

^bMedian (10th percentile, 90th percentile).

^cBetween group analysis was performed on natural log-transformed values due to a non-normal distribution of this characteristic.

^dPercentage of patients with the WMH subtype on MRI in the group of patients with lacunes, without lacunes and in the total study population.

^eIn periventricular or confluent WMHs, a lower convexity, and a higher solidity, concavity index or fractal dimension corresponds to a more complex lesion. In deep WMH, a higher eccentricity corresponds to a more round lesion, while a lower eccentricity corresponds to a more elongated lesion. A higher fractal dimension of a deep lesion corresponds to a more complex lesion.

Table 3. Results of linear regression analyses with lacunes on MRI as independent variable and total, periventricular or confluent WMH, and deep WMH volumes as dependent variables (all natural log-transformed).

	Total B (95% CI) ^a	Periventricular or confluent B (95% CI) ^a	Deep B (95% CI) ^a
No lacunes on MRI	0 (reference)	0 (reference)	0 (reference)
Lacunes on MRI	1.03 (0.86 to 1.21) ^b	1.08 (0.89 to 1.27) ^b	0.71 (0.44 to 0.97) ^b

WMH: white matter hyperintensity; MRI: magnetic resonance imaging; CI: confidence interval.

^aAdjusted for age, sex and total intracranial volume. B represents the natural log-transformed difference in volume between patients with and without lacunes on MRI.

^bp < 0.0001.

In patients with a confluent WMH subtype, presence of lacunes was associated with a more complex WMH shape (lower convexity Z-score (B = -0.46, 95% CI: -0.74 to -0.19) and a higher concavity index Z-score (B = 0.65, 95% CI: 0.33 to 0.97)) after adjusting for age and sex. These associations remained statistically

significant after additionally adjusting for total WMH volume (B = -0.29, 95% CI: -0.55 to -0.04; B = 0.30, 95% CI: 0.10 to 0.50, respectively), indicating that patients with lacunes had a more complex WMH shape independent of WMH volume. Patients with multiple lacunes did not show a different WMH

Table 4. Results of Poisson regression with WMH subtype groups as dependent variable and lacunes on MRI as independent variable (n = 188).

	Patients with a periventricular WMH subtype without deep WMHs (n = 360)	Patients with a periventricular WMH subtype with deep WMHs (n = 424)	Patients with a confluent WMH subtype (n = 215)
	RR (95% CI)	RR (95% CI) ^a	RR (95% CI) ^a
Lacunes vs. no lacunes	1 (reference)	1.41 (1.22 to 1.62)	2.41 (1.98 to 2.92)

WMH: white matter hyperintensity; RR: relative risk; CI: confidence interval.

^aAdjusted for age, sex and total intracranial volume.

shape compared to patients with one lacune (convexity Z-score $B=0.03$, 95% CI: -0.34 to 0.40 , concavity index Z-score $B=0.17$, 95% CI: -0.13 to 0.46), after adjusting for age, sex, and total WMH volume. No differences were found for the remaining WMH shape features between patients with one lacune and patients with multiple lacunes. Presence of lacunes was associated with higher fractal dimension Z-scores ($B=0.28$, 95% CI: 0.09 to 0.47) compared to absence of lacunes, after adjusting for age and sex. However, this association attenuated and lost statistical significance after additionally adjusting for total WMH volume ($B=0.04$, 95% CI: -0.05 to 0.13). No statistically significant associations were found between presence of lacunes, and eccentricity and fractal dimension of deep WMHs in patients with a confluent WMH subtype.

In patients with a periventricular WMH subtype with deep WMHs, presence of lacunes was associated with lower solidity Z-scores ($B=-0.25$, 95% CI: -0.47 to -0.02) and higher fractal dimension Z-scores ($B=0.18$, 95% CI: 0.01 to 0.36) compared to absence of lacunes, after adjusting for age and sex. This indicates more irregular shaped WMHs in patients with lacunes; however, the associations lost statistical significance after additionally adjusting for total WMH volume ($B=-0.04$, 95% CI: -0.20 to 0.11 , $B=-0.01$, 95% CI: -0.09 to 0.08 , respectively). Presence of lacunes was not associated with eccentricity and fractal dimension of deep WMHs in these patients. WMH shape features did not differ between patients with one lacune and patients with multiple lacunes in this group.

Presence of lacunes was associated with lower solidity Z-scores ($B=-0.48$, 95% CI: -0.83 to -0.13) in patients with a periventricular WMH subtype without deep WMHs, after adjusting for age and sex. After additionally adjusting for total WMH volume, this relationship attenuated and lost statistical significance ($B=-0.20$, 95% CI: -0.44 to 0.05). WMH shape features did not differ between patients with one lacune and patients with multiple lacunes in this group.

Discussion

In this cohort of patients with a history of vascular disease, we observed that patients with lacunes on MRI had greater total, periventricular or confluent, and deep WMH volumes than patients without lacunes. Patients with lacunes also had an increased risk of confluent type WMHs and deep WMHs. Finally, patients with lacunes had a more irregular shape of confluent WMHs than patients without lacunes, independent of total WMH volume.

Our results regarding WMH volume are in line with the findings of a prior cross-sectional MR study that used quantitative WMH volume measurements.²³ In this study, greater total WMH volumes were found in patients with lacunar stroke than in non-lacunar stroke subtypes in two independent cohorts of patients with ischemic stroke.²³ However, more recent studies have shown that lacunar stroke is not synonymous with lacunes, and conversely not all lacunes are due to lacunar stroke.^{5,24-27} Therefore, it is likely that patients with lacunes in our study represent a more heterogeneous group of small vessel pathologies than solely lacunar stroke, and the results should be interpreted accordingly. In addition to the previous study,²³ we showed that WMH subtype and WMH shape features are also associated with lacunes. To the best of our knowledge, these WMH features have not been previously linked to the presence of lacunes on brain MRI.

Although small vessel pathologies are considered the culprit for both lacunes and WMHs, previous studies have shown that the pathological processes leading to WMHs and lacunes are diverse.²⁸⁻³⁰ For example, it is thought that not all lacunes are due to lacunar infarcts.⁵ Rather, a lacune most likely represents damage to the brain from different etiologies, such as small hemorrhages, infarcts, microembolism, amyloid angiopathy, or arteritis.^{2,26} While it is currently impossible to determine the specific underlying small vessel pathologies in individual patients using brain MRI, several possibilities can be proposed that may explain the association between lacunes and WMH volume and subtype. First,

Table 5. Linear regression analyses of WMH shape parameters as dependent variables and lacunes on MRI as independent variable.

WMH subtype groups ^b	Solidity periventricular or confluent WMHs (Z-score) ^a	Convexity periventricular or confluent WMHs (Z-score) ^a	Concavity index periventricular or confluent WMHs (Z-score) ^a	Fractal dimension periventricular or confluent WMHs (Z-score) ^a	Fractal dimension deep WMHs (Z-score) ^a	
						B (95% CI) ^c
Patients with a periventricular WMH subtype with deep WMHs (n=424)	Model 1	-0.25 (-0.47 to -0.02)*	0.17 (-0.09 to 0.44)	-0.03 (-0.19 to 0.14)	0.18 (0.01 to 0.36)*	-0.22 (-0.52 to 0.07)
	Model 2	-0.04 (-0.20 to 0.11)	0.01 (-0.22 to 0.24)	-0.01 (-0.17 to 0.16)	-0.01 (-0.09 to 0.08)	-0.19 (-0.49 to 0.11)
Patients with a periventricular WMH subtype without deep WMHs (n=360)	Model 1	-0.48 (-0.83 to -0.13)*	0.35 (-0.06 to 0.75)	-0.15 (-0.44 to 0.13)	0.32 (-0.02 to 0.65)	NA
	Model 2	-0.20 (-0.44 to 0.05)	0.09 (-0.24 to 0.42)	-0.03 (-0.30 to 0.26)	-0.01 (-0.18 to 0.17)	NA
Patients with a confluent WMH subtype (n=215)	Model 1	-0.11 (-0.26 to 0.04)	-0.46 (-0.74 to -0.19)*	0.65 (0.33 to 0.97)*	0.28 (0.09 to 0.47)*	-0.02 (-0.20 to 0.16)
	Model 2	0.02 (-0.10 to 0.13)	-0.29 (-0.55 to -0.04)*	0.30 (0.10 to 0.50)*	0.04 (-0.05 to 0.13)	-0.03 (-0.20 to 0.15)

WMH: white matter hyperintensity; ICV: intracranial volume; NA: not applicable; CI: confidence interval.

^aIn periventricular or confluent WMH, a lower convexity, and a higher solidity, concavity index or fractal dimension corresponds to a more complex lesion. In deep WMH, a higher eccentricity corresponds to a more round lesion, while a lower eccentricity corresponds to a more elongated lesion. A higher fractal dimension of a deep lesion corresponds to a more complex lesion.

^bLinear regression analyses were performed separately in each WMH subtype group.

^cB represents difference in WMH shape parameter for patients with lacunes versus those without lacunes.

Model 1: Adjusted for age and sex. Model 2: Additionally adjusted for natural log-transformed total WMH volume (% ICV).

**p* < 0.05.

it may be that lacunes and WMHs share a common pathogenesis, while at the same time not affecting each other.^{5,24} Alternatively, WMHs may lead to the formation of lacunes through secondary hypoperfusion and ischemia in the surrounding brain parenchyma.³¹ This notion has been supported by a recent study in patients with an inherited form of CSVD in which the edges of WMHs were identified as a predilection site for lacunes.³² Also, lacunes may promote formation of WMHs, possibly through affecting white matter tract integrity.³³ With regard to WMH shape, we found that lacunes are associated with more irregular WMHs in patients with confluent lesions independent of WMH volume. Previous histopathological studies have demonstrated that more irregular periventricular and confluent WMHs correspond to more severe small vessel changes.⁷⁻⁹ While it may be that lacunes in the presence of irregular confluent WMHs indicate increasing CSVD severity, it should be acknowledged that the relationship between WMH shape features as measured in our study and clinical outcomes are currently not known. To the best of our knowledge, our study is the first to quantify periventricular, confluent and deep WMH shape features on brain MRI, and further work is needed to examine whether WMH shape features are associated with clinical outcomes.

Our findings might have clinical relevance. Previous studies have shown that WMHs and lacunes have consistently been associated with cognitive and functional impairment.^{11,15,16} The strong association between lacunes and WMHs in our study suggests that lacunes may affect clinical outcomes not only through their own presence¹³ but also through the concomitant presence of WMHs and vice versa. In addition, our results indicate that WMH volume and subtype should be considered as possible confounders in analyses investigating the relationship between lacunes and clinical outcomes.

We found in our study that patients with lacunes were older, more often had diabetes mellitus and hypertension, and had a higher IMT than patients without lacunes. These observations support findings of two large population-based studies in which increased age, hypertension, and diabetes mellitus were found to be associated with presence of lacunes on MRI.^{34,35} It has been hypothesized that diabetes mellitus and hypertension may lead to lipohyalinosis and microatheroma formation, respectively, in the microvasculature of the brain.^{4,24} As discussed above, these processes can lead to acute lacunar infarcts, large acute infarcts or small hemorrhages, which eventually can lead to formation of lacunes.^{4,5,26} Thus, our findings add to the notion that certain vascular risk factors may be associated with lacunes, and future research is warranted to investigate whether diabetes mellitus and/or hypertension

may act as possible targets for prevention or treatment of CSVD.²⁴

Although in our study patients with multiple lacunes showed a greater WMH volume than patients with only one lacune, we did not find differences for WMH subtype or WMH shape. Taken together, our data suggest that the association between lacunes and WMHs is largely determined by the presence of lacunes, rather than the number of lacunes. While this finding may support the notion that WMHs and lacunes result from the same underlying mechanism, future studies in different cohorts are needed to validate our findings with respect to the impact of the amount of lacunes on WMH features.

The strengths of our study are the use of a large cohort of patients in which we used quantitative WMH volume measurements and automated image processing techniques to examine multiple features of WMHs and their relation to lacunes. Also, we adjusted our shape analyses for total WMH volume to determine to what extent a more irregular shape of WMH was explained by a greater WMH volume.

A limitation of our study is the cross-sectional design, which did not allow us to assess the relationship between lacunes and WMH features over time. Another limitation might be the use of a somewhat arbitrary distance of 10 mm from the margins of the lateral ventricles to differentiate periventricular from confluent WMHs. It should be noted, however, that there are currently no unambiguous, non-disputable approaches to differentiate periventricular from confluent WMHs, and some authors have proposed a distance of 10 mm.³⁶ Lastly, our study consisted of patients with a history of vascular disease, which may limit the generalizability of the results. However, this characteristic of our study cohort may also have led to a higher prevalence of lacunes and greater total WMH volumes,³⁷ which facilitated the analyses.

In conclusion, we found that lacunes on MRI were associated with several WMH features that correspond to more severe small vessel changes, mortality, and poor functional outcomes.

Project members

We gratefully acknowledge the contribution of the SMART research personnel: R. van Petersen and B.G.F. Dinther and also the participants of the SMART Study Group: A. Algra MD, PhD; Y. van der Graaf, MD, PhD; D.E. Grobbee, MD, PhD; G.E.H.M. Rutten, MD, PhD, Julius Center for Health Sciences and Primary care; F.L.J. Visseren, MD, PhD, Department of Internal Medicine; G.J. de Borst, MD, PhD, Department of Vascular Surgery; L.J. Kappelle, MD, PhD, Department of Neurology; T.

Leiner, MD, PhD, Department of Radiology; P.A. Doevendans, MD, PhD, Department of Cardiology.

Funding

The author(s) disclosed receipt of the following financial support for the research, authorship, and/or publication of this article: Funding for this paper was received as part of a grant from the Netherlands Organization for Scientific Research-Medical Sciences (NWO-MW: project no. 904-65-095). This funding source had no role in the design, data collection, data analyses and data interpretation of the study or writing of the report. We also gratefully acknowledge the funding from the European Research Council under the European Union's Horizon 2020 Programme (H2020)/ERC grant agreement nos. °637024 and 66681 (SVDs@target).

Declaration of conflicting interests

The author(s) declared no potential conflicts of interest with respect to the research, authorship, and/or publication of this article.

Authors' contributions

Rashid Ghaznawi – Literature search, figures, data collection, MR image processing, data analysis, data interpretation, and writing.

Mirjam I Geerlings – Study design, data interpretation, and critically reviewed the manuscript.

Myriam G Jaarsma-Coes – MR image processing and analysis, data analysis, and critically reviewed the manuscript.

Maarten HT Zwartbol – Data interpretation and critically reviewed the manuscript.

Hugo J Kuijf – MR image processing and analysis, critically reviewed the manuscript.

Yolanda van der Graaf – Study design, critically reviewed the manuscript.

Theo D Witkamp – MR image analysis, critically reviewed the manuscript.

Jeroen Hendrikse – Critically reviewed the manuscript.


Jeroen de Bresser – Data interpretation and critically reviewed the manuscript.

Supplementary material

Supplementary material for this paper can be found at the journal website: <http://journals.sagepub.com/home/jcb>

ORCID iD

Myriam G. Jaarsma-Coes  <http://orcid.org/0000-0003-3423-9370>

Hugo J. Kuijf  <http://orcid.org/0000-0001-6997-9059>

References

- Makin SD, Turpin S, Dennis MS, et al. Cognitive impairment after lacunar stroke: systematic review and meta-analysis of incidence, prevalence and comparison with other stroke subtypes. *J Neurol Neurosurg Psychiatry* 2013; 84: 893–900.
- Ostergaard L, Engedal TS, Moreton F, et al. Cerebral small vessel disease: capillary pathways to stroke and cognitive decline. *J Cereb Blood Flow Metab* 2016; 36: 302–325.
- Pantoni L, Poggesi A and Inzitari D. Cognitive decline and dementia related to cerebrovascular diseases: some evidence and concepts. *Cerebrovasc Dis* 2009; 27(Suppl 1): 191–196.
- Wardlaw JM, Smith C and Dichgans M. Mechanisms of sporadic cerebral small vessel disease: insights from neuroimaging. *Lancet Neurol* 2013; 12: 483–497.
- Wardlaw JM, Smith EE, Biessels GJ, et al. Neuroimaging standards for research into small vessel disease and its contribution to ageing and neurodegeneration. *Lancet Neurol* 2013; 12: 822–838.
- Lambert C, Benjamin P, Zeestraten E, et al. Longitudinal patterns of leukoaraiosis and brain atrophy in symptomatic small vessel disease. *Brain* 2016; 139: 1136–1151.
- Gouw AA, Seewann A, van der Flier WM, et al. Heterogeneity of small vessel disease: a systematic review of MRI and histopathology correlations. *J Neurol Neurosurg Psychiatry* 2011; 82: 126–135.
- Fazekas F, Kleinert R, Offenbacher H, et al. Pathologic correlates of incidental MRI white matter signal hyperintensities. *Neurology* 1993; 43: 1683–1689.
- Kim KW, MacFall JR and Payne ME. Classification of white matter lesions on magnetic resonance imaging in elderly persons. *Biol Psychiatry* 2008; 64: 273–280.
- Fazekas F, Kleinert R, Offenbacher H, et al. The morphologic correlate of incidental punctate white matter hyperintensities on MR images. *AJNR Am J Neuroradiol* 1991; 12: 915–921.
- Prins ND and Scheltens P. White matter hyperintensities, cognitive impairment and dementia: an update. *Nat Rev Neurol* 2015; 11: 157–165.
- Griffanti L, Jenkinson M, Suri S, et al. Classification and characterization of periventricular and deep white matter hyperintensities on MRI: a study in older adults. *Neuroimage* 2018; 170: 174–181.
- Conijn MM, Kloppenborg RP, Algra A, et al. Cerebral small vessel disease and risk of death, ischemic stroke, and cardiac complications in patients with atherosclerotic disease: the Second Manifestations of ARterial disease-Magnetic Resonance (SMART-MR) study. *Stroke* 2011; 42: 3105–3109.
- DeBette S and Markus HS. The clinical importance of white matter hyperintensities on brain magnetic resonance imaging: systematic review and meta-analysis. *BMJ* 2010; 341: c3666.
- Jokinen H, Gouw AA, Madureira S, et al. Incident lacunes influence cognitive decline: the LADIS study. *Neurology* 2011; 76: 1872–1878.
- Benisty S, Gouw AA, Porcher R, et al. Location of lacunar infarcts correlates with cognition in a sample of non-disabled subjects with age-related white-matter changes: the LADIS study. *J Neurol Neurosurg Psychiatry* 2009; 80: 478–483.
- Andersen SD, Skjoth F, Yavarian Y, et al. Multiple silent lacunes are associated with recurrent ischemic stroke. *Cerebrovasc Dis* 2016; 42: 73–80.

18. de Bresser J, Kuijff HJ, Zaanen K, et al. White matter hyperintensity shape and location feature analysis on brain MRI; proof of principle study in patients with diabetes. *Sci Rep* 2018; 8: 1893.
19. Geerlings MI, Appelman AP, Vincken KL, et al. Brain volumes and cerebrovascular lesions on MRI in patients with atherosclerotic disease. The SMART-MR study. *Atherosclerosis* 2010; 210: 130–136.
20. Anbeek P, Vincken KL, van Bochove GS, et al. Probabilistic segmentation of brain tissue in MR imaging. *Neuroimage* 2005; 27: 795–804.
21. Kempton MJ, Underwood TS, Brunton S, et al. A comprehensive testing protocol for MRI neuroanatomical segmentation techniques: evaluation of a novel lateral ventricle segmentation method. *Neuroimage* 2011; 58: 1051–1059.
22. Liu EJ, Cashman KV and Rust AC. Optimising shape analysis to quantify volcanic ash morphology. *GeoResJ* 2015; 8: 14–30.
23. Rost NS, Rahman RM, Biffi A, et al. White matter hyperintensity volume is increased in small vessel stroke subtypes. *Neurology* 2010; 75: 1670–1677.
24. Pantoni L. Cerebral small vessel disease: from pathogenesis and clinical characteristics to therapeutic challenges. *Lancet Neurol* 2010; 9: 689–701.
25. Potter GM, Doubal FN, Jackson CA, et al. Counting cavitating lacunes underestimates the burden of lacunar infarction. *Stroke* 2010; 41: 267–272.
26. Wardlaw JM. What is a lacune? *Stroke* 2008; 39: 2921–2922.
27. Wardlaw JM, Sandercock PA, Dennis MS, et al. Is breakdown of the blood-brain barrier responsible for lacunar stroke, leukoaraiosis, and dementia? *Stroke* 2003; 34: 806–812.
28. Ogata J, Yutani C, Otsubo R, et al. Heart and vessel pathology underlying brain infarction in 142 stroke patients. *Ann Neurol* 2008; 63: 770–781.
29. Ogata J, Yamanishi H and Ishibashi-Ueda H. Review: role of cerebral vessels in ischaemic injury of the brain. *Neuropathol Appl Neurobiol* 2011; 37: 40–55.
30. Eng JA, Frosch MP, Choi K, et al. Clinical manifestations of cerebral amyloid angiopathy-related inflammation. *Ann Neurol* 2004; 55: 250–256.
31. Gouw AA, van der Flier WM, Pantoni L, et al. On the etiology of incident brain lacunes: longitudinal observations from the LADIS study. *Stroke* 2008; 39: 3083–3085.
32. Duering M, Csanadi E, Gesierich B, et al. Incident lacunes preferentially localize to the edge of white matter hyperintensities: insights into the pathophysiology of cerebral small vessel disease. *Brain* 2013; 136: 2717–2726.
33. Reijmer YD, Freeze WM, Leemans A, et al. The effect of lacunar infarcts on white matter tract integrity. *Stroke* 2013; 44: 2019–2021.
34. Bezerra DC, Sharrett AR, Matsushita K, et al. Risk factors for lacune subtypes in the Atherosclerosis Risk in Communities (ARIC) Study. *Neurology* 2012; 78: 102–108.
35. Longstreth WT Jr, Bernick C, Manolio TA, et al. Lacunar infarcts defined by magnetic resonance imaging of 3660 elderly people: the Cardiovascular Health Study. *Arch Neurol* 1998; 55: 1217–1225.
36. DeCarli C, Fletcher E, Ramey V, et al. Anatomical mapping of white matter hyperintensities (WMH): exploring the relationships between periventricular WMH, deep WMH, and total WMH burden. *Stroke* 2005; 36: 50–55.
37. Jackson CA, Hutchison A, Dennis MS, et al. Differing risk factor profiles of ischemic stroke subtypes: evidence for a distinct lacunar arteriopathy? *Stroke* 2010; 41: 624–629.